General Disclaimer

One or more of the Following Statements may affect this Document

- This document has been reproduced from the best copy furnished by the organizational source. It is being released in the interest of making available as much information as possible.

- This document may contain data, which exceeds the sheet parameters. It was furnished in this condition by the organizational source and is the best copy available.

- This document may contain tone-on-tone or color graphs, charts and/or pictures, which have been reproduced in black and white.

- This document is paginated as submitted by the original source.

- Portions of this document are not fully legible due to the historical nature of some of the material. However, it is the best reproduction available from the original submission.

Produced by the NASA Center for Aerospace Information (CASI)

NAGW-92

C S S A

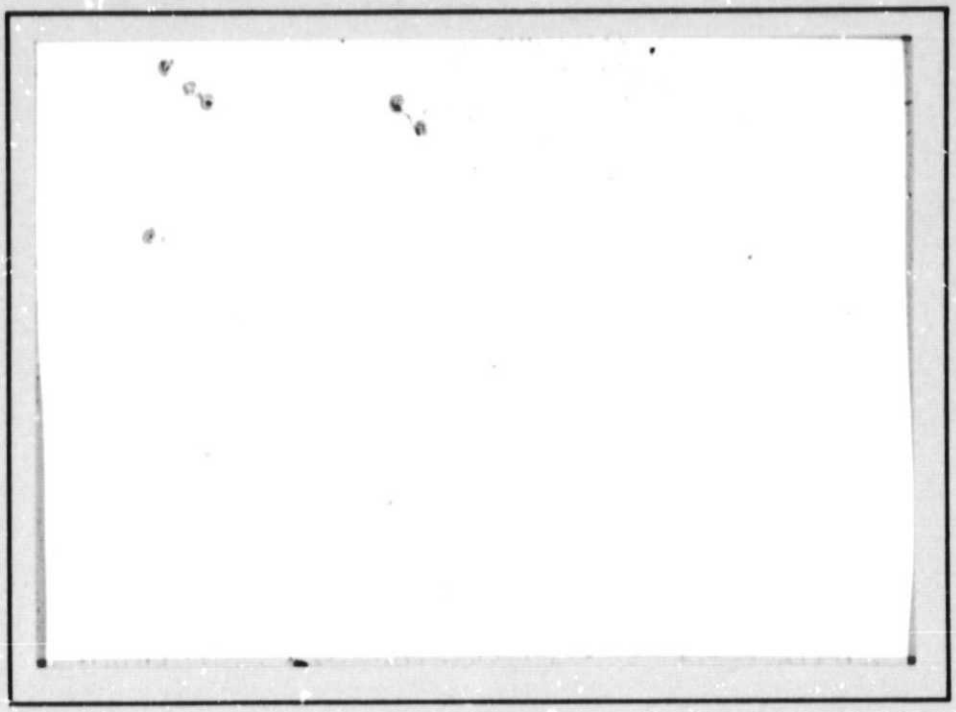

CENTER FOR SPACE SCIENCE AND ASTROPHYSICS
STANFORD UNIVERSITY
Stanford, California

(NASA-CR-175495) THERMAL STABILITY OF STATIC CORONAL LOOPS: PART 1: EFFECTS OF BOUNDARY CONDITIONS (Stanford Univ.) 42 p HC A03/MF A01 CSCL 03B

N85-22330

Unclas G3/92 14430

THERMAL STABILITY OF STATIC CORONAL LOOPS: I. EFFECTS OF BOUNDARY CONDITIONS

S. K. Antiochos and E. C. Shoub
Center for Space Science and Astrophysics
Stanford University

C.-H. An*
Center for Astrophysics and Space Science
University of California-San Diego

A. G. Emslie
Department of Physics
University of Alabama

CSSA-ASTRO-85-14
March 1985

NATIONAL AERONAUTICS AND SPACE ADMINISTRATION
Grant NGL 05-020-272
Grant NAGW-92
Grant NGR 05-020-668

OFFICE OF NAVAL RESEARCH
Contract N00014-85-K-0111

NSG 7401
ONR NSF

*Current address: NASA-Marshall Space Flight Center

Abstract

We investigate the linear stability of static coronal-loop models undergoing thermal perturbations. The effect of conditions at the loop base on the stability properties of the models is considered in detail. We consider the question of appropriate boundary conditions at the loop base and conclude that the most physical assumptions are that the temperature and density (or pressure) perturbations vanish there. However, if the base is taken to be sufficiently deep in the chromosphere, either several chromospheric scale heights or several coronal loop lengths in depth, then the effect of the boundary conditions on loop stability becomes negligible so that all physically acceptable conditions are equally appropriate. For example, one could as well assume that the velocity vanishes at the base.

We calculate the growth rates and eigenmodes of static models in which gravity is neglected and in which the coronal heating is a relatively simple function, either constant per-unit mass or per-unit volume. We find that all such models are unstable with a growth rate of the order of the coronal cooling time. The physical implications of these results for the solar corona and transition region are discussed.

I. Introduction

For some time now static models of coronal loops (e.g., Rosner, Tucker, and Vaiana 1978; Craig, McClymont, and Underwood 1978; Vesecky, Antiochos, and Underwood 1979) have been widely used to interpret observations of both solar and stellar coronae (e.g., Bonnett and Dupree 1980, Orrall 1981). The key assumption in these models is that the energy input to the corona is constant in time so that a static solution to the relevant equations is possible. However, even if a static solution is mathematically possible, it will not be physically realizable unless this solution is also stable to small amplitude perturbations. It is well known that the coronal plasma is susceptible to a thermal instability due to the form of the dependence of radiative loss rate on temperature (Field 1965). Therefore, in order to assess their degree of validity, it is necessary to determine whether the static models are thermally stable or unstable.

The linear theory for the thermal stability of static coronal-loop models has been investigated by a number of authors, but with differing conclusions. In his original work, Antiochos (1979) concluded that the static models were thermally unstable. Similar results were obtained by Hood and Priest (1980). However, Chiuderi, Einaudi, and Torricelli-Ciamponi (1981); Craig and McClymont (1981); and McClymont and Craig (1981a,b,c) have found that the models are either stable or that the growth rates for instability are too small to be physically significant. The origin of this difference in the results of the two sets of authors is in their treatment of the base of the loop models. Antiochos (1979) and Hood and Priest (1980) have not included cool material, $T \lesssim 10^5$ K, in their model, for which the form of radiative loss curve (e.g., Raymond, Cox, and Smith 1976) favors linear stability (Field 1965). In addition, Antiochos

has considered only perturbations with a vanishing first-order heat flux at the base. Chiuderi, Einaudi and Torricelli-Ciamponi; and Craig and McClymont argue that the growth rates for instability are very sensitive to these assumptions so that the models can be effectively stabilized either by including chromospheric material in the model (Craig and McClymont 1981) or by changing the boundary conditions so that the temperature perturbation, instead of the heat-flux perturbation, is assumed to vanish at the base (Chiuderi, Einaudi, and Torricelli-Ciamponi 1981).

The reason for this apparently high sensitivity of the models to the base conditions lies in one of the well-known properties of the static models: the fact that the magnitude of the conduction and radiation terms in the energy balance are approximately equal throughout the loop (Vesecky, Antiochos, and Underwood 1978). As discussed by Field (1965), we expect thermal instability in coronal plasma whose structure is such that radiation dominates. On the other hand, we expect stability if the structure is conduction dominated, since conduction always acts to damp out any temperature perturbation. Hence, the static models, whose structure is such that these two terms are comparable, are perched near the boundary separating stability from instability. Even seemingly minor changes on the form of the base or of the boundary conditions at the base can be sufficient to push the models to one side or the other of this boundary.

It is clear, therefore, that the proper treatment of the base is critical for determining to what extent the models are either stable or unstable. In the next section we discuss the question of the base conditions in detail. In Sections III and IV we calculate growth rates and eigenmodes for various static models and for various boundary conditions. In the final section, V, we discuss the implications of our results.

II. Boundary Conditions

As an aid to determining the appropriate boundary conditions, let us first write down the perturbation equations for a one-dimensional loop model. Assuming that all physical variables are of the form:

$$f(s,t) = f_0(s) + e^{\nu t} f_1(s) \quad , \tag{1}$$

and assuming that the growth or damping time $1/\nu$ is slow compared to the sound travel time so that the acceleration terms can be neglected in the momentum equation, we obtain (Field 1965, Antiochos 1979):

$$\nu n_1 + \frac{1}{A}\frac{d}{ds}(An_0V_1) = 0 \tag{2}$$

$$\frac{d}{ds} P_1 = m\, n_1\, g_{||} \tag{3}$$

$$3/2(\nu p_1 + V_1 \frac{d}{ds} P_0) - 5/2 \frac{P_0}{n_0}(\nu n_1 + V_1 \frac{d}{ds} n_0) + \frac{1}{A}\frac{d}{ds}(AF_1) = \mathcal{L}_1 \tag{4}$$

and

$$\frac{P_1}{P_0} = \frac{n_1}{n_0} + \frac{T_1}{T_0} \quad , \tag{5}$$

where: $A(s)$ is the cross-sectional area of the loop; $g_{||}(s)$ is the component of gravity parallel to the loop; F_1 is the perturbed heat flux, which for the Spitzer (1962) conductivity is given explicitly by:

$$F_1 = -10^{-6} \frac{d}{ds}(T_0^{5/2} T_1) \quad . \tag{6}$$

$\mathcal{L}_1$ constitutes the perturbed energy sources and sinks of the plasma. For optically thin radiative losses and for a coronal heating function that depends only on density and temperature or, equivalently, pressure and temperature, $\mathcal{L}_1$ is given explicitly by (Antiochos 1979):

$$\mathcal{L}_1 = -2n_0 n_1 \Lambda(T_0) - n_0^2 \frac{d\Lambda}{dT_0} T_1 + \frac{\partial \varepsilon}{\partial P_0} P_1 + \frac{\partial \varepsilon}{\partial T_0} T_1 \quad , \tag{7}$$

where $\Lambda(T)$ is the radiative loss coefficient (e.g., Cox and Tucker 1969) and $\varepsilon(p,T)$ is the coronal heating rate. The equilibrium profiles are, of course, given by (e.g., Vesecky, Antiochos, and Underwood 1979):

$$\frac{d}{ds} P_0 = m\, n_0\, g_{||} \tag{8a}$$

$$\frac{-10^{-6}}{\Lambda} \frac{d}{ds} \left(\Lambda T_0^{5/2} \frac{dT_0}{ds} \right) = \mathcal{L}_0 = -n_0^2 \Lambda(T_0) + \varepsilon(P_0, T_0) \quad . \tag{8b}$$

Note that we have neglected in equations (2) - (8) effects due to changes in ionization equilibrium or to optically thick radiation, both of which are clearly important in the chromosphere. Hence, this model cannot be used to determine the stability of the true solar chromosphere. We use this model chromosphere only for investigating the effect of having thermally stable material at the base of the corona and transition region. Since our results will turn out to be insensitive to the detailed structure of this region, we expect that our analysis will also be applicable to the solar chromosphere as long as it is thermally stable as well.

It is evident from the equations above that there are four independent spatial derivatives in the problem, which implies that four boundary conditions are required. This is to be expected since the full nonlinear equations also require four spatial boundary conditions for a unique solution (e.g., Richtmyer and Morton 1967). The usual situation is that at end of the loop two boundary conditions are specified. One condition generally relates to the thermal properties of the base; for example, with respect to the perturbation the loop base may act as a thermal bath, in which case the appropriate condition is that the temperature perturbation vanishes there, $T_{1b} = 0$; or it may act as a thermal insulator so that the

perturbation heat flux vanishes there, $F_{1b} = 0$. The other condition generally relates to the inertial properties of the base; for example, it may act as a rigid wall with respect to the perturbation so that the velocity vanishes, $V_{1b} = 0$, or a "free surface," so that the pressure perturbation, $P_{1b} = 0$. Most of the discussion in the literature has concerned these four conditions, and the discussion in this paper will also concentrate on these four. Let us emphasize, however, that there are an infinite number of other possible boundary conditions and that, lacking some physical justification, there is no reason to single out the four above. A priori, all conditions are equally acceptable.

There has also been a considerable discussion in the literature on the distinction between symmetric and antisymmetric modes. However, this distinction is spurious. It is due only to the special class of models considered by the previous authors (Antiochos 1979; Hood and Priest 1980; Chiuderi, Einaudi, and Torricelli-Ciamponi 1981; Craig and McClymont 1981). In their models gravity is neglected, and the loop area and the coronal heating do not have any spatial variation. Under these simplifications, the static equations are autonomous, and the equilibrium models are symmetric about the loop apex. Hence, the solutions to the first-order equations, i.e., the normal modes of the loop, are either purely symmetric or antisymmetric about the apex. These results will clearly not hold for a realistic equilibrium model that has no special symmetry properties. For such a model each choice of four boundary conditions will, in general, determine a complete and distinct set of eigenvalues and eigenfunctions. Within each set all the modes are equally valid. Hence, in this paper we will avoid any discussion in terms of symmetric or antisymmetric modes; and since the most important mode from the viewpoint of thermal instability is the lowest order one, we will concentrate on the fundamental.

The question remains as to what choice of boundary conditions best represents the physical situation at the base of a solar loop. Ideally, one would like conditions at the loop base not to affect the stability properties of the corona and transition region. The standard procedure for achieving this is to place the base sufficiently far that over the time scale of any instability no effects can propagate to the base. However, the sound travel time in the corona, chromosphere and even photosphere is very rapid compared to typical thermal time scales, such as the coronal cooling time. On this time scale, material at the loop base is always in contact with the coronal plasma, even if the base is assumed to be in the photosphere. Note that our neglect of the acceleration terms in the force equation is tantamount to assuming an infinite sound speed and, consequently, a negligible propagation time scale throughout the loop. For such a model it is not obvious, at least to us, whether the position of the base can ever be chosen so that conditions there have an insignificant effect on the behavior of the corona. We show below that, fortunately, even with the rapid sound speed, the base has a negligible influence on the coronal stability if it is placed sufficiently deep.

In order to determine the physically valid boundary conditions to impose at the loop base, we need a definite model for this base region. As a simple model let us assume that the chromosphere below a coronal loop is isothermal at temperature T_b, is in hydrostatic equilibrium, and is strictly stable. In addition, we assume there is no real end point to a solar loop, so this model base region extends below the corona and transition region to arbitrarily large depths, i.e., either to many chromospheric scale heights or to depths large compared to the coronal loop length. Finally, let us neglect the curvature of the loop for this analysis and set $g_{||}(s)$ to be a constant.

The form of the boundary conditions follows simply from the requirement that, since we are interested in coronal disturbances, the perturbations should vanish or at least remain finite in the chromosphere. Combining equations (3) and (5), an expression can be obtained for the pressure perturbation P in terms of the temperature perturbation T_1 :

$$\frac{P_1(s)}{P_0(s)} = \frac{P_1(0)}{P_0(0)} - \int_0^s \frac{T_1}{T_0} \frac{ds}{H(T_0)} \quad , \tag{9}$$

where H (T_0) is the gravitational scale height at temperature T_0:

$$H(T) \equiv \frac{2kT}{mg_{||}} \tag{10}$$

and s = 0 is some reference point in the loop (the top is convenient). We are defining s to increase downwards. It is evident from (9) that in order for $P_1(s)$ to remain finite with increasing depth in the chromosphere, i.e., s -> ∞, the temperature perturbation must vanish with depth T_1 -> 0. In fact, T_1 must decay quite rapidly with depth, on the size scale of the chromospheric scale height $H(T_b)$ or less, because the equilibrium pressure P_0 grows exponentially on this size scale. Note that we are excluding the possibility of modes that oscillate indefinitely with depth. We are interested primarily in the lowest order mode; and as we will see below, this usually has no zero crossings.

We conclude, therefore, that the proper thermal boundary condition is that T_{1b}= 0. This result is to be expected physically. It follows from the fact that any perturbation of the temperature also implies a perturbation of the gravitational scale height. If the temperature disturbance extends more than a scale height or so deep into the atmosphere, a very large pressure disturbance must result due to the change in scale height. Hence, the only physically acceptable temperature perturbations are those that vanish on the order of a scale height or less.

Now, to determine the inertial boundary condition, we integrate the continuity equation (2) to obtain an expression for the particle flux $n_0 V_1$ in terms of the density perturbation n_1:

$$n_0(s)V_1(s) = n_0(0)\ V_1(0) - \nu\int_0^s n_1\ ds \quad . \tag{11}$$

As in the situation above, it is evident that in order for $n_0 V_1$ to remain finite as $s \to \infty$, n_1 must vanish with depth. Again, this is to be expected physically. If the density disturbance extends over a large depth, then the change in the total number of particles in this region must be large, and consequently a large flux of particles into or out of the region must result. It is evident from (11) that in the chromosphere n_1 must vanish faster than L_c/s, where L_c is the size scale of the coronal portion of the loop, i.e., the region where we expect a finite n_1. Note that the density perturbation may extend to much greater depths than the temperature one. We found above that T_1 must vanish at least as fast as $\exp(-s/H_b)$, where H_b is the gravitational scale height in the chromosphere. For typical solar loops $H_b \ll L_c$.

We conclude that the proper boundary conditions at the loop base are that $T_{1b} = 0$ and $n_{1b} = 0$. At any finite depth this is equivalent to the set $T_{1b} = 0$ and $P_{1b} = 0$. Although the temperature, density, and pressure perturbations vanish, the mass flux does not. Using (2) and (3), the perturbed mass flux can be related to the pressure perturbation:

$$n_0 V_1 = n_0(0)\ V_1(0) - \frac{\nu}{mg_{||}}\ (P_1(s) - P_1(0)) \quad . \tag{12}$$

Since the pressure perturbation vanishes with depth, the mass flux will in general tend to some finite constant, corresponding to a steady-state flow in the chromosphere and below. This is to be expected on physical grounds as well. We do not expect the temperature and density structure deep in

the chromosphere or photosphere to be affected by a disturbance in the corona. However, if as in our problem, the time scale of the disturbance is long compared to the sound travel time, then a steady flow must occur at large depths to support any coronal flows. Of course, the velocity itself, V_1, vanishes with depth since the density n_0 increases; however, the mass flux $n_0 V_1$ stays constant. This is exactly the situation that we found for the case of evaporative cooling of coronal loops (Antiochos and Sturrock 1978). There again, the coronal evolution occurred on time scales long compared to the sound travel time, and it was found that a steady flow was set up at the loop base due to evaporative motions in the corona. This is also the situation for the photosphere at the base of an open magnetic field region such as in a coronal hole. In these regions coronal heating results in a steady solar wind flow. The presence of this flow has no observable effect on photospheric temperatures and pressures, but it clearly implies the existence of a mass flux in the photosphere equal to the coronal mass flux.

Let us now examine the effect of using different boundary conditions at the loop base, in particular, the rigid-wall one. We wish to find out how the coronal perturbation depends on the base conditions, for example, how $P_1(0)$ depends on $n_{0b} V_{1b}$. From (12) it is evident that specifying the base mass flux is equivalent to specifying the base pressure perturbation, but the relation between $P_1(0)$ and P_{1b} is given by (9):

$$P_1(0) = \frac{P_0(0)}{P_{0b}} P_{1b} + P_0(0) \int_0^L \frac{T_1}{T_0} \frac{ds}{H(T_0)} \quad . \tag{13}$$

Equation (13) is the key result. The effect on the coronal perturbation $P_1(0)$ of assuming a non-vanishing P_{1b} is given by the first term on the right-hand side of (13). This term is of order $P_0(0)/P_{0b}$ for a temperature perturbation that vanishes rapidly in the chromosphere so that the pressure

perturbation there is of order the coronal one (i.e., $P_1(s)$ does not diverge exponentially in the chromosphere). For a base that is several scale heights deep, $P_0(0)/P_{0b}$ is negligible; therefore, the form of the coronal perturbation is insensitive to the boundary condition on P_{1b}or, equivalently, V_{1b}.

The situation is clarified by Figure 1, where for a given $T_1(s)$ we plot the resulting form of $P_1(s)$ and $n_0V_1(s)$ for both rigid-wall $V_{1b} = 0$ and free-surface $P_{1b} = 0$ boundary conditions. Since this is for illustrative purposes only, we have taken an extremely simple equilibrium loop model in which we neglect the effects of gravity in the corona and assume that the transition region is vanishingly thin. The corona is, therefore, isothermal and isobaric and is defined to extend from $s = 0$ to $s = L_c$. Below this corona is an isothermal chromosphere in hydrostatic equilibrium and with a temperature 100 times lower. The base of the loop model is taken to occur 10 chromospheric scale heights deep, $L = L_c + 10\ H_b$. For simplicity, the temperature perturbation, T_1/T_0, is assumed to be constant in the corona and to decay exponentially in the chromosphere on a size scale of $H_b/10$.

The forms for $P_1(s)$ and $n_0V_1(s)$ obtained from (9) and (11) are plotted in Figure 1a and 1b, respectively. We have taken the velocity to vanish at the top, $V_1(0) = 0$, which would be the case for the lowest order mode of a symmetric loop model. On the scale of this figure, the modes with $P_{1b} = 0$ and those with $V_{1b} = 0$ are indistinguishable except within a few scale heights of the base. In this boundary region the rigid wall mass flux exhibits a sudden decrease to zero, and P_1 exhibits a sudden increase back up to its coronal value, i.e., $P_{1b} = P_1(0)$. Note that the magnitude of this jump does not change with position of the base. No matter how deep the rigid wall is placed, there will occur a small boundary layer at the

wall where the pressure P_{1b} jumps back up to its coronal value. The physical reason for this is straightforward. Flows in the corona will cause material either to pile up or to evacuate from the wall. Hence, there must exist a pressure gradient near the wall of the same order as the coronal gradient in order to decelerate or accelerate the flows. However, over most of the chromosphere the flows are in a steady state, and the pressure perturbation is negligible.

It is clear from these results that the appropriate boundary condition to assume at the loop base is that $P_{1b} = 0$. This condition results naturally in the chromosphere, irrespective of what is assumed at the base as long as the base is placed sufficiently deep. If the base is placed within several scale heights of the top of the chromosphere, then it is the only boundary condition that is appropriate; the use of rigid-wall conditions, or any others, is likely to lead to incorrect conclusions. If the base is placed many scale heights deep, then the particular boundary condition used becomes irrelevant.

III. Analytic Results

a) Perturbation Equations

In this paper we calculate growth rates and eigenfunctions only for the simplified problem discussed by previous authors; we neglect gravity and any spatial variation in the loop area or heating function. We discuss the effects of gravity and the area variation in a subsequent paper (Antiochos and An 1985). For purposes of comparison, we calculate the growth rates and modes for several sets of boundary conditions, although as we discussed above, the physically appropriate ones are $T_{1b} = 0$ and $n_{1b} = 0$.

Under the special assumptions above, the perturbation equations (2) - (6) can be simplified to a form essentially equivalent to the one we used previously (Antiochos 1979):

$$\frac{d}{dx}\left(y\,\frac{d}{dx}\mu\right) + Q(x)\mu + \lambda\mu = \eta\, G(x) \quad , \tag{14}$$

where we have defined dimensionless variables:

$$x = s/L \quad , \tag{15}$$

L is the loop half-length,

$$y(x) \equiv \left(T_0/T_0(0)\right)^{7/2} \quad , \tag{16}$$

$$\mu \equiv \frac{y^{5/14}}{\nu}\,\frac{d}{ds}\,v_1 \quad , \tag{17}$$

and $\eta = \dfrac{P_1}{P_0}$ = constant. (18)

The eigenvalue λ is defined as:

$$\lambda = -\left(L/L_c\right)^2 \nu\,\tau \quad , \tag{19}$$

where τ is given by the coronal cooling time scale

$$\tau = \frac{5}{2}\cdot 10^6\, P_0\, L_c^2\, \left(T_0\,(0)\right)^{-7/2} \quad . \tag{20}$$

The functions Q(x) and G(x) are given by:

$$Q(x) = \frac{1}{14}\,\frac{d^2y}{dx^2} - \frac{1}{y}\left(\frac{5}{14}\,\frac{dy}{dx}\right)^2 + \alpha\left(T_0\,\frac{\partial \mathcal{L}}{\partial T_0}\right) \tag{21a}$$

$$G(x) = -y^{5/14}\left(3/5\,\lambda + \frac{d^2y}{dx^2} + \alpha T_0\,\frac{\partial \mathcal{L}}{\partial T_0} + \alpha P_0\,\frac{\partial \mathcal{L}}{\partial P_0}\right) \quad . \tag{21b}$$

where α is a constant of the dimensions:

$$\alpha = 10^6\, L^2\, \left(T_0(0)\right)^{-7/2} \tag{22}$$

The boundary conditions must now be specified. Assuming the "natural" ones, $n_{1b} = T_{1b} = 0$ leads to:

$$\eta = 0 \quad \text{and} \quad \mu_b = 0 \tag{23}$$

at each end of the loop. Note that we have used the fact that the equilibrium heat flux vanishes at the base in order to derive Equation (23). If one assumes instead the rigid-wall conditions $V_{1b} = T_{1b} = 0$, this leads to the constraint (Antiochos 1979):

$$\int_0^1 \mu \, y^{-5/14} \, dx = 0 \tag{24a}$$

and the conditions:

$$\mu_b + y_b^{5/14} \eta = 0 \quad . \tag{24b}$$

With this formulation it is difficult to compare the effects of the two sets of boundary conditions since one set leads to homogeneous conditions on μ, (23), whereas the other does not. In order to facilitate the comparison, let us for the moment reformulate the problem in terms of a new variable defined as $\zeta = \mu + y^{5/14}\eta$, so that the boundary conditions (24b) will become homogeneous. Hence, the problem reduces to solving an equation for ζ and η of the form (14) (only the form of G(x) changes) and with boundary conditions:

for free surface, $\zeta_b = 0$, and $\eta = 0$;

for rigid wall, $\zeta_b = 0$, and $\eta = \int_0^1 \zeta \, y^{-5/14} \, dx$. (25)

The relation between the two sets of conditions is now transparent. We note that if, as expected, ζ decreases sufficiently rapidly in the chromosphere, then (24) implies that in the limit of large chromospheric depths, i.e., $L_c/L \to 0$,

$$\eta \to (L_c/L) \langle \zeta \, y^{-5/14} \rangle \quad , \tag{26}$$

where the brackets indicate the average coronal value. Hence, for large depths, η decays as L_c/L. This is the same behavior that we found before, except that now since there is no gravity, the only scale in the problem is the coronal loop length, so that this length rather than the gravitational scale height determines the decay scale for the effects of the wall.

b) Asymptotic Forms

In order to check whether ζ will, in fact, decrease rapidly in the chromosphere, let us examine the asymptotic forms for ζ in this region as predicted by equation (14). We first consider the free-surface case. Since T_0 is approximately constant in the chromosphere, Equation (14) reduces to:

$$y_b \frac{d^2}{dx^2} \zeta_f + \alpha \left(T_0 \frac{\partial \mathcal{L}}{\partial T_0} \right)_b \zeta_f - \left(\frac{L}{L_c} \right)^2 \nu_f \tau \zeta_f = 0 \quad , \tag{27}$$

where the subscript "f" is used to refer to the free-surface variables. Assuming that the radiative loss function has a simple power-law dependence on T, and that the power is positive so that the chromosphere is radiatively stable, then we expect that:

$$\left(\frac{T_0}{P_0} \frac{\partial \mathcal{L}}{\partial T_0} \right)_b \sim - \frac{\mathcal{L}}{P_0} \sim - 1/\tau_b \quad , \tag{28}$$

where τ_b is the radiative cooling time at the base. Note that our definition for $\mathcal{L}$ has a sign change from that used by Field (1965) and that the negative sign is required for stability. Assuming that the free-surface growth rate, ν_f, is of order the coronal cooling rate $1/\tau$, Equations (27) and (28) yield the following asymptotic form for ζ,

where

$$\zeta \sim e^{-s/\ell}$$

$$\ell \approx L_c \left(\frac{T_b}{T_0(0)} \right)^{7/4} (1 + \tau/\tau_b)^{-1/2} \quad . \tag{29}$$

The longest length scale for the decay is obtained in the limit $\tau/\tau_b \rightarrow 0$. This length, $\sim L_c (T_b/T_0(0))^{7/4}$, is typically small compared to physical size scales either in the corona or chromosphere. We show below that the form predicted above is obtained from exact solution of (14).

We now consider the rigid-wall case. With ζ_r as the dependent variable, Equation (14) becomes:

$$\frac{d}{dx}\left(y \frac{d}{dx} \zeta_r\right) + Q(x)\, \zeta_r + \lambda_r \zeta_r = \eta_r (\lambda_r f(x) + g(x)) \quad , \tag{30}$$

where the subscript "r" is used to indicate rigid-wall quantities. The functions f and g are given by:

$$f(x) = \frac{2}{5} y^{5/14} \tag{31}$$

and

$$g(x) = -y^{5/14} \left(\frac{4}{7} \frac{d^2 y}{dx^2} + \alpha P_0 \frac{\partial \mathcal{L}}{\partial P_0} \right) . \tag{32}$$

Following the arguments above, in the base region, Equation (30) reduces to:

$$\begin{aligned} y_b \frac{d^2}{dx^2} \zeta_r - \left(\frac{L}{L_c}\right)^2 \frac{\tau}{\tau_b} \zeta_r - \left(\frac{L}{L_c}\right)^2 \tau\, \nu_r\, \zeta_r \\ \approx \eta_r\, y_b^{5/14} \left(\frac{L}{L_c}\right)^2 \left(-\frac{2}{5} \nu_r \tau + \tau/\tau_b\right) \quad , \end{aligned} \tag{33}$$

where, again, due to the form of the radiative losses, we assume that:

$$\left(\frac{\partial \mathcal{L}}{\partial P_0}\right)_b \sim -1/\tau_b \quad . \tag{34}$$

The general solution to (33) consists of a linear combination of the homogeneous and particular solutions. However, the homogeneous solution is equivalent to the free-surface solution, and we found above that this decays exponentially. Hence, the solution at large depths is dominated by

the particular solution:

$$\zeta_r \to \frac{2}{5}\,\eta_r\, y_b^{5/14}\,\frac{(\nu_r\,\tau_b - 5/2)}{(\nu_r\,\tau_b + 1)} \quad . \tag{35}$$

If, as expected, $\nu_r \sim O(1/\tau)$, then for $\tau/\tau_b \to 0$

$$\zeta_r \to \frac{2}{5}\,\eta_r\, y_b^{5/14} \quad . \tag{36}$$

We will see below that (35) also agrees with exact solution of (14).

These results verify our claim that η_r decays as L_c/L. We have that

$$\eta_r = \int_0^{L_c/L} \zeta_r\, y^{-5/14}\, dx + \int_{L_c/L}^{1} \zeta_r\, y^{-5/14}\, dx \quad . \tag{37}$$

Substituting the asymptotic form (35), or (36), into the second integral yields (26) to within a factor of order unity.

The effect on the growth rate of imposing a rigid-wall constraint can also be estimated. Using the equations for ζ_f and ζ_r, and their boundary conditions, the following expression is obtained:

$$\delta\lambda = \lambda_r - \lambda_f = \frac{\lambda_f \int_0^1 \zeta_f\, f(x)\, dx + \int_0^1 \zeta_f\, g(x)\, dx}{\int_0^1 \frac{\zeta_f \zeta_r}{\eta_r}\, dx - \int_0^1 \zeta_f\, f(x)\, dx} \quad . \tag{38}$$

If $L_c/L \ll 1$, then to lowest order in L_c/L, Equation (38) can be written as:

$$\delta\nu = \nu_r - \nu_f = \left(\frac{\int_0^1 \zeta_f\, y^{-5/14}\, dx}{\int_0^1 \zeta_f^2\, dx} \right) \int_0^1 y^{5/14}\, \zeta_f \frac{2}{5} \left(\nu_f - \frac{2\mathcal{L}}{P_0} + \frac{\partial \mathcal{L}}{\partial P_0} \right) dx \quad . \tag{39}$$

Each of the integrals in (39) is of order L_c/L; hence, $\delta\nu$ is also of this order.

Depending on the sign of $\delta\nu$, the rigid-wall can have a stabilizing ($\delta\nu$ negative) or destabilizing ($\delta\nu$ positive) influence. Since ζ_f, the lowest

order mode, has no zero crossings and its normalization is irrelevant, the sign of $\delta\nu$ is determined primarily by the sign of the terms in the brackets in the rightmost integral; however, this factor does not have a unique sign. The first term ν_f is always positive and for models of interest has magnitude ~ $1/\tau$; consequently, it enhances instability. The sum of the second and third term is proportional to $(-\varepsilon/P_0)$ for the case where the heating ε is constant per particle, and $(-2\varepsilon/P_0)$ for ε constant per unit volume. Hence, the contribution from the last two terms is negative, and since in the static model the energy input and the radiative losses are roughly equal in the corona (e.g., Vesecky, Antiochos, and Underwood 1979), ε/P_0 is also of order $1/\tau$. It is, therefore, not clear which of the two contributions will dominate; however, it turns out that the negative contribution is usually larger than the positive one so that the rigid wall has a net stabilizing effect.

This is to be expected physically. A rigid wall acts to inhibit flows and, consequently, any density disturbance. For optically thin radiation at coronal temperatures, both the temperature dependence and the density dependence of the losses is such as to promote instability (Field 1965). By suppressing the density effect, a rigid wall tends to weaken the instability. It is interesting to note that this need not always be the case. Sometimes a rigid wall can actually enhance instability. In particular, if ν_f is very large and dominates the other terms in (39), we would expect $\delta\nu$ to be positive. This situation does occur for models in which the base is placed high up in the transition region and the temperature boundary condition is assumed to be $dT_{1b}/ds = 0$. For such

models the growth time $1/\nu_f$ is very short, of order the cooling time in the transition region rather than that in the corona (Antiochos 1979). We find that for these cases the rigid-wall growth rate ν_r is slightly larger than ν_f. However, for models in which some cool stable material occurs at the base, the rigid-wall boundary conditions always result in smaller growth rates.

IV. Numerical Results

The mathematical problem that must be solved is now clearly defined. For the free-surface conditions, (14) reduces to a standard Sturm-Liouville problem, as in Antiochos (1979), which we solve in exactly the same manner as before.

For the rigid-wall conditions, the inhomogeneous problem must be solved subject to the constraint (24a). Note that this is not a standard Sturm-Liouville problem; hence, none of the well-known theorems (e.g., Morse and Feshbach 1953) on the behavior of the eigenfunctions and eigenvalues need apply. There are two parameters, λ and η, that must be determined; therefore, we do not use a "shooting" technique as in the homogeneous case to obtain solutions. First, we note that since η will, in general, be non-zero for any finite-length loop, we can eliminate it by defining a new dependent variable (μ/η). Now (14) and (24a) define a nonlinear boundary-value problem for (μ/η) and the unknown parameter λ. This is solved by standard techniques: Newton-Raphson iteration and finite-difference solution of the linearized equations. Convergence was rapid, $\lesssim 20$ iterations for all the cases we investigated.

One numerical complication is the extreme variation in temperature scale height between the corona, the transition region, and the

chromosphere. This makes it impossible to use a uniform grid for finite differencing the independent variable x. However, we cannot use the equilibrium temperature T_0 as the independent variable since the temperature gradient vanishes at the loop apex and base. Instead, we define a new independent variable r:

$$dr = \left(\frac{T_0(0)}{T_0}\right)^2 \left(1-\left(1-\frac{T_b}{T_0(0)}\right)\frac{T_b}{T_0}\right)^2 dx \qquad (40)$$

and use a uniform grid in r. It is evident from (30) that the effect of transforming to r is to increase the number of grid points at transition region temperatures ($T_0(0) < T_0 < T_b$) by a factor of order $(T_0(0)/T_0)^2$. We found that this was sufficient to yield an accurate solution.

a) Form of Heating and Cooling

There are two functions in the problem that have yet to be specified: the radiative loss coefficient, $\Lambda(T)$, and the energy input rate $\epsilon(n,T)$. For the former we use a smooth analytic approximation to the curve derived by Raymond, Cox and Smith (1976). Figure 2 shows this curve along with our approximation to it. The stability properties of the models are not sensitive to the exact form of $\Lambda(T)$ as long as this form is such that it implies radiative instability above ~ 10^5 K and stability below.

Since the mechanism for coronal heating is not known, the form of the energy input ϵ is essentially arbitrary. In our previous work we found that the stability properties are insensitive to the exact form for ϵ, at least, for the case where this form is a power-law dependence on n and T. Hence, we simply assume that in the corona and transition region the energy input either per unit volume or per particle is constant. At lower temperatures a different form for the energy input must be used in order to have a significant mass of material at "chromospheric" temperature,

$T < 5 \times 10^4$ K. In order for the model to have a large chromosphere, the temperature gradients and, hence, the heat flux must be small at these temperatures. The radiation losses in the chromosphere cannot be balanced by conduction from above (e.g., Athay 1981); thus for a static model these losses must be balanced by the energy input (e.g., Craig, Robb and Rollo 1982).

Therefore, we use the following form for the energy input:

$$\varepsilon = Qn^{\gamma} \tanh(\chi(T)) + n^2\Lambda(1 - \tanh(\chi(T))) \quad , \tag{41}$$

where

$$\chi(T) = C\,(T/T_b - 1 + \delta)^m \tag{42}$$

and Q, γ, C, m and δ are constants. Equations (41) and (42) imply that for $\delta << 1$:

$$\varepsilon \rightarrow \begin{cases} Qn^{\gamma}, & \text{for } T > T_b \\ n^2\Lambda, & \text{for } T = T_b \end{cases} \quad , \tag{43}$$

i.e., the energy input rate tends to Qn^{γ} for temperatures larger than the base temperatures and tends to the radiative loss rate at the base temperature. The values 0 and 1 for γ correspond to constant coronal heating per unit volume and per unit mass, respectively. The depth of material at the base temperature is determined by the value of δ; it becomes arbitrarily large for arbitrarily small δ.

The form that we assume for the energy input, (41) and (42) may appear highly unphysical because it undegoes an abrupt although continuous change near $T = T_b$. However, such a sharp structure in the energy input rate is implied by the observations. Empirical models of the upper chromosphere,

such as the VAL models (Vernazza, Avrett and Loesser 1981), all indicate the presence of a flat temperature "plateau" at $T \sim 2 \times 10^4$ K with a very abrupt rise at higher temperatures. Within the context of the static model, and neglecting possible kinetic effects (Shoub 1983), the only way to obtain the observed very sharp structure in the temperature profile is to have a correspondingly sharp structure in the energy input rate. This is one reason why the static models are generally assumed to have a base above 2×10^4 K. The particular form, (41) and (42) is chosen simply for convenience. It permits us to investigate the effects of adding a varying amount of cool, radiatively stable material to the loop base.

b) Growth Rates

(i) Free Surface

We have calculated the eigenvalues λ for a wide range of static models. In particular, we have determined the dependence of the stability on the following properties of the model: the coronal temperature, the base temperature, the depth of the chromosphere, the form for the heating and, of course, the boundary conditions. The main result of this analysis is that for the boundary conditions $T_{1b} = 0$, $n_{1b} = 0$, all the models were unstable with a growth time approximately equal to the coronal cooling time. The growth rate was found to be completely insensitive to the loop temperature either in the corona or base, to the amount of chromospheric material or to the form of the chromospheric heating. Hence, we conclude that the instability is a true physical one and will occur in solar loops that satisfy our basic assumptions, i.e., spatial variations in the loop area and heating, and the effects of gravity can be neglected.

Figure 3 shows the growth rate $\nu\tau$ of the lowest free-surface mode

obtained by solving (14) for a series of static models with different base properties. These static models all have very similar coronal properties. The apex temperature $T_0(0)$ was chosen in each case to be 10^6 K and the coronal heating given by $\gamma = 1$ and $Q = 10^{-12}$ ergs/sec/particle, equation (41). Given the coronal temperature and heating rate, then as is well known (e.g., Vesecky, Antiochos, and Underwood 1979), the coronal density and coronal loop length are constrained by the scaling laws. They turn out to be $n_0(0) = 3.2 \times 10^9$ cm^{-3} and $L_c = 5.2 \times 10^8$ cm. Conditions at the base, however, are very insensitive to the coronal conditions, so that we can vary the base temperature and the amount of base material with almost no change in coronal parameters.

In our model the base temperature is given by T_b, and the depth of the chromosphere is determined primarily by the constant δ, equation (43). Hence, there are actually two distinct sets of models in Figure 3. In one set all the models have a value of $\delta \equiv 1$, which implies that there is an insignificant amount of material at the base. These models correspond to the usual static-loop models, as in Vesecky, Antiochos, and Underwood (1979). For such models we investigated the effect of the base temperature on stability by varying T_b from 2×10^5 K to 10^4 K. In Figure 3 only the cases down to $T_b = 3 \times 10^4$ K are shown, but no change was observed in using T_b down to 10^4. As is clear from the figure, the value of the base temperature has essentially no effect on loop stability. The growth rate $\nu\tau$ is of order unity irrespective of whether T_b is chosen to occur at chromospheric or transition-region temperatures.

The second set of models in Figure 3 are those with a fixed base temperature $T_b = 3 \times 10^4$ K, but with varying amounts of base material at this temperature. The value of δ was varied from $\delta = 1$ to $\delta = 5 \times 10^{-6}$. The other parameters in the energy input rate (equation (42)) were fixed,

C = 10 and m = 3. This value for m is convenient numerically since for m = 3 the depth of the base region turns out to be proportional to $1/\delta$; hence, the range of chromospheric depths covered by the range used for δ is correspondingly large, $(L - L_c)/L_c$ ranges from ~ 10^{-5} to ~ 10. Again, we note that there is almost no variation in ν irrespective of the depth of the chromosphere.

We have investigated the effect of the form of the coronal heating on stability by performing a series of calculations as in Figure 3 for the case of uniform heating per unit volume, $\gamma = 0$. The results are essentially identical to those shown in Figure 3. This agrees with our previous calculations (Antiochos 1979) in which we investigated a wide range of values for γ and found no significant effect on the growth rate.

We have also looked for any possible effect due to the form of the chromospheric heating by varying the exponent m defined in (43). This parameter determines the degree of stability of the chromosphere, i.e., the magnitude of the quantity $(T_0 \partial \mathcal{L}/\partial T_0)$ (cf., Field 1965). The chromospheric magnitude of this quantity is small in our models compared to its coronal value except for the case m = 1. Note that for m = 1 the chromospheric depth $L - L_c$ varies only as $\ln(1/\delta)$ so that even with the smallest value of δ usable numerically, ~ 10^{-15}, the chromospheric depth is not large, $(L - L_c)/L_c$ ~ .05. The results for the cases with m = 1 are identical to those shown in Figure 3 for the case m = 3. Again, there is no significant dependence of the growth rate ν on either the base temperature or the chromospheric depth. We conclude that the instability does not depend on the particular form, (42), that we assumed for the chromospheric heating.

This result is to be expected. For temperatures $\lesssim 5 \times 10^4$ K, the quantity $T_0 \frac{\partial \mathcal{L}}{\partial T_0}$ is strictly negative in all our models; hence, this region cannot contribute to any instability. As we will see below, the unstable

modes have a vanishingly small amplitude in this region compared to coronal amplitudes.

(ii) Rigid Wall

We have solved Equation (14) for the rigid-wall conditions (24) and for the exact wide range of equilibrium models used with the free-surface conditions. Some of the results are shown in Figure 3. The growth rate of the lowest rigid-wall mode is plotted for comparison with the corresponding free-surface mode. The rigid-wall rate is seen to approach the free-surface one as the chromospheric depth becomes large, $L_c/L \ll 1$; the ratio of the growth rates is near unity, $\nu_r/\nu_f = .85$ for the deepest model in the figure, $L_c/L = .07$. These numerical results confirm the analytic arguments above that for large depths the rigid-wall condition is equivalent to the free-surface one.

We find that the rigid-wall growth rates are also insensitive to the coronal temperature, the base temperature or the form of the heating. However, Figure 3 shows that they do depend on the depth of the base region. For models with $L_c \gtrsim L/2$, the growth rate is negative, indicating stability. Note that this value for L_c/L actually implies a large chromospheric region. Since the base density is approximately two orders of magnitude greater than the coronal density, the bulk of the loop plasma is in the base for $L_c/L = .5$. Note also that the damping rate is almost constant for models with $\delta \gtrsim 10^{-2}$. This result emphasizes the unphysical nature of the rigid-wall conditions and the danger in using them. If one assumes the rigid-wall condition and then considers models with increasing chromospheric depths, it first appears that static loops are stable and that the stability is insensitive to base conditions. One would naturally conclude that the models are physically stable. But as the base depth is

increased, the models suddenly become unstable. Somehow the addition of too much stable material at the base destabilizes the corona! This is clearly an unphysical result and is due to using improper assumptions at the onset.

The same type of behavior is found when boundary conditions other than $T_{1b} = 0$ and $n_{1b} = 0$ are used. For example, Craig and McClymont (1981) find that the conditions $dT_{1b}/ds = 0$ and $P_{1b} = 0$ lead to abrupt changes in the growth rate at very small chromospheric depths. We have also examined these conditions and a variety of others defined by the vanishing of a linear combination of T_{1b} and F_{1b} or P_{1b} and V_{1b}. Depending on the particular equilibrium model, the boundary conditions assumed can result in growth rates either larger or smaller than the free surface one; however, in all cases the rates tended to the free-surface result for large chromospheric depths. In all but the free-surface case the growth rates exhibited an abrupt change at some range of chromospheric depth; hence, the conditions $T_{1b} = n_{1b} = 0$ are the <u>only</u> ones that are generally valid.

c) <u>Normal Modes</u>

Along with the eigenvalues λ we have also calculated the eigenfunctions μ for all the equilibrium models considered. Two representative cases are shown in Figures 4a and 4b. In Figure 4a we show both the free-surface T_1/T_0 and the rigid-wall mode, $T_1/\eta T_0$, for the equilibrium model of Figure 3 with the deepest chromosphere ($L_c/L = .07$ corresponding to $\delta = 5 \times 10^{-6}$). In Figure 4b the results for the model with $\delta = 10^{-3}$, ($L_c/L = .97$), are shown.

We first discuss the results for the deepest model, Fig. 4a. In order to resolve their structure in the transition region, the modes are plotted against a nonlinear distance scale. From the loop apex, s = 0, to a point

two coronal depths down, $s = 2L_c$, the equilibrium temperature T_0 is used as the independent variable. From this depth down to the loop base, $s = L$, the distance itself is used. Of course, all the significant structure in the eigenmodes occurs well above the point $s = 2L_c$. The region below this depth is included in the figure only to point out that the numerical calculations verify the analytic asymptotic forms obtained above. Using (29) and taking $\tau/\tau_b = 0$, we find that the decay scale ℓ for the free-surface mode is equal to $2.16 \times 10^{-3} L_c$. Hence, the free-surface mode should have essentially zero amplitude in the deep region. The numerical results agree with this. We find that the amplitude of T_1/T_0 drops below computer accuracy well before $s = 2L$. On the other hand, the amplitude of the rigid-wall mode, $T_1/\eta T_0$, does not vanish. Instead, it has a constant value of 0.4 over most of the chromosphere and vanishes only near the base on the size scale ℓ. This behavior is also in agreement with the analytic results. In the chromosphere, $T_1/\eta T_0 = \zeta/\eta y^{5/14}$; therefore, from (36) we expect the mode to approach the value 2/5, except very near the base, where it must vanish due to the boundary conditions.

It can be seen from Fig. 4a that the modes have significant amplitude only in the corona and transition region. The free-surface mode has been normalized to equal the rigid-wall value at the apex. Note that the rigid-wall quantity $T_1/\eta T_0$ does not have an aribtrary normalization factor since this quantity is the ratio of the temperature-to-pressure perturbations. Its magnitude has physical significance. Our results indicate that the pressure perturbation is in the same sense but smaller than the temperature perturbation. As the depth of the chromospheric region increases, $L_c/L \to 0$, we find that the coronal magnitude of $T_1/\eta T_0$ increases as $(L_c/L)^{-1}$. This confirms our previous result that η should decrease as L_c/L for a fixed temperature perturbation.

On the scale of Fig. 4a the two modes are almost identical in the corona and transition region. Only near the base is there a significant deviation; and as the depth of the base region is increased, the two modes become indistinguishable. The modes exhibit a stong peak near 5×10^4 K. At approximately this temperature the radiative losses change from being a destabilizing to a stabilizing effect, so that below this temperature the modes decay very rapidly on the scale of ℓ. It is important to emphasize that although the modes peak strongly in the transition region, the instability is not a local one. The modes have finite amplitude throughout the corona, and the growth rates correspond to the coronal cooling time rather than the much faster cooling time in the transition region. Hence, the instability is a global one involving the complete loop except for the chromosphere.

The situation is somewhat different for the model with a shallower base, Fig. 4b. The free-surface mode is very similar to that of the model. with the deeper base. Indeed, this mode is insensitive to just about everything; hence, the curve shown in Fig. 4a (or 4b) can be considered the universal form.

However, the rigid-wall mode is obviously very different from that of Fig. 4a. The most striking difference is that the mode has a zero crossing at the base of the transition region and is negative in the chromosphere. This is in agreement with the analytic results. We note from (35) that as ν decreases from a large positive quantity, the asymptotic amplitude becomes negative. As ν decreases further to a large negative quantity, the amplitude becomes positive again. The numerical results agree with the behavior. For models with large depths, $\delta \lesssim 10^{-4}$, the amplitude in the chromosphere is positive. For models with intermediate depths, $\delta \sim 10^{-3}$, it is negative. It becomes positive again for small depths, $\delta > 10^{-2}$. For

models without a very deep base, the chromospheric form of the rigid-wall mode is clearly quite sensitive to the exact position of the wall. The free-surface mode, on the other hand, shows no change for all values of δ that we investigated.

In the corona the rigid-wall mode has the same general shape as that in Fig. 4a, but the amplitude is an order of magnitude smaller. This means that for a given amplitude temperature perturbation, the effect of the decrease in the base depth is an increase in the coronal pressure perturbation by an order of magnitude. In fact, the pressure perturbation actually has a larger coronal amplitude than the temperature perturbation. We note from Fig. 4b that the ratio of the temperature to pressure amplitude is less than unity for temperatures down to ~ 8×10^5 K. This region encompasses about 70 percent of the coronal portion of the loop. Since from (5)

$$\frac{T_1}{T_0 \eta} + \frac{n_1}{n_0 \eta} = 1 \quad , \tag{44}$$

our results imply that over most of the croona the temperature and density perturbations must be in the same sense. A decrease (an increase) in the temperature is accompanied by a decrease (an increase)in the density as well. Since a decrease in the temperature implies an increase in the radiative loss rate (for $T > 10^5$ K), whereas a decrease in the density implies a decrease in the losses, the perturbations oppose each other as far as instability is concerned. The net result is stability, $\nu < 0$ for the model in Fig. 4b. For models with a deeper base region, as in Fig. 4a, the temperature perturbation is much larger than the pressure perturbation, and, consequently, the density perturbation takes the opposite sense. Both the temperature and density disturbances act to promote instability, and the model of Fig. 4a is, indeed, unstable, $\nu > 0$. We conclude that the

stability of the rigid-wall models such as Fig. 4b is a boundary-condition effect. It is due solely to the assumption of a rigid-wall at a particular depth.

V. Discussion

There are two key results of this paper. The first is that the appropriate boundary conditions to assume at the loop base are $T_{1b} = n_{1b} = 0$. For models with a sufficiently deep base ($L_b >> \min(H_b, L_c)$), all boundary conditions can be used; however, the set above is the only one that is appropriate for models that do not satisfy this condition. Indeed, we find it surprising just how universally valid these boundary conditions appear to be. Even for models with little or no chromosphere, they yield the correct growth rate and form of the eigenmode for the instability. Contrary to the conclusions of several authors (Habbal and Rosner 1979; Chiuderi, Einaudi, and Torricelli-Ciamponi 1981; Craig and McClymont 1981; and McClymont and Craig 1981a, b, c), the mere presence of radiatively stable material at the loop base does not stabilize the static models. If incorrect boundary conditions are used, then the base can act either to stabilize or, as we showed above, to destabilize the static models. However, if the proper conditions are used, then the amount of base material has no effect on the stability.

This is a convenient result from a numerical point of view. It is often quite difficult to handle numerical models with extremely deep base regions (e.g., Craig, Robb, and Rollo 1982). Our results indicate that models with very shallow bases can yield correct results if the correct boundary conditions are used.

The second main result of this paper is that under our assumptions,

static models of coronal loops are thermally unstable. The growth rate of the instablity is of the order the coronal cooling time (20). The basic assumptions that we made for the equlibrium models were that gravity and all spatial variations in the loop area or heating rate are negligible. These are the most commonly used assumptions in calculating static models. An important question is: how sensitive are our results to these assumptions? McClymont and Craig (1981a,b,c) have considered the question of spatial variations in the heating rate. They find that these can act either to enhance or to damp instability. Lacking a model for the coronal heating process, nothing definitive can be stated on this issue; hence, we will not consider it further. We will discuss the effects of gravity and the area variation in a forthcoming appear. In general, the area variation acts to enhance the instability; however, we do not expect it to enhance the growth rates to values much beyond the ones here, since these are already of the order of the coronal cooling rate. Gravity, on the other hand, acts to damp the instability (e.g., Wragg and Priest 1982); hence, our results are certain to apply only for loops in which gravity can be neglected.

We can identify at least two possible physical situations in the solar corona where the effects of gravity should be small so that our results clearly apply. One is the case of loops sufficiently low lying, heights $\lesssim$ 1000 km, so that the loop height is smaller than any gravitational scale height in the loop. Another is the case of magnetic field lines that are concave in the corona, so that near the loop center the force of gravity is directed toward the center rather than away from it, as in the usual case. This is the type of magnetic geometry believed to be responsible for quiescent prominences. Our results imply that these two types of structures are naturally unstable without any special requirements on the

coronal heating process. We believe that the thermal instability discussed in this paper is responsible for the cool material that is often observed to occur in the corona.

Of course, in order to prove this statement, the nonlinear development of instability must be calculated. Clearly, the instability must not saturate at a low amplitude if it is to produce observational effects in the corona. Only the linear growth rates were considered in this paper; the nonlinear evaluation must be determined by numerical simulation. Numerical simulations of coronal loops have been performed by several authors (e.g., Craig, Robb, and Rollo 1982; Peres et al. 1982; Oran, Mariska, and Boris 1982). These simulations have not exhibited any significant evidence for thermal instability; however, to our knowledge no one has considered models in which the effects of gravity are negligible and the correct boundary conditions are employed at the loop base. Our results indicate that the instability should be present in such models. We intend to investigate the nonlinear stability of coronal loops in a future work.

Acknowledgments

The work at Stanford was supported by NASA Grants NGL 05-020-272 and NAGW-92 and ONR Contract N00014-85-K-0111 (formerly N00014-75-C-0673). The work at UCSD was supported by NASA Grant NSG-7406. Acknowledgment is made to the National Center for Atmospheric Research, which is sponsored by the National Science Foundation, for some of the computer time used in this research.

References

Antiochos, S. K. 1979, Ap. J. (Letters), 232, L125.

Antiochos, S. K., and An, C.-H. 1985, Ap. J. (to be submitted).

Athay, R. G. 1981, in Solar Phenomena in Stars and Stellar Systems (eds. R. M. Barnett and A. K. Dupree; Boston: D. Reidel), p. 173.

Bonnett, R. M., and Dupree, A. K. 1980, Solar Phenomena in Stars and Stellar Systems (Dordrecht: D. Reidel).

Chiuderi, C., Einaudi, G., and Torricelli-Ciamponi, G. 1981, Astron. Ap., 97, 27.

Cox, D. P., and Tucker, W. H. 1969, Ap. J., 157, 1157.

Craig, I. J. D., and McClymont, A. N. 1981, Nature, 294, 333.

Craig, I. J. D., McClymont, A. N., and Underwood, J. H. 1978,

Craig, I. J. D., Robb, T. D., and Rollo, M. D. 1982, Sol. Phys., 76, 331.

Field, G. B. 1965, Ap. J., 142, 531.

Habbal, S. R., and Rosner, R. 1979, Ap. J., 234, 1113.

Hood, A. W., and Priest, E. R. 1980, Astron. Ap., 87, 126.

McClymont, A. N., and Craig, I. J. D. 1981a, Univ. of Waikato Math. Res. Report No. 96.

_____. 1981b, Univ. of Waikato Math. Res. Report No. 99.

_____. 1981c, Univ. of Waikato Math. Res. Report No. 100.

Morse, P. M., and Feshbach, H. 1953, Methods of Theoretical Physics (New York: McGraw-Hill), Ch. 6.

Oran, E. S., Mariska, J. T., and Boris, J. P. 1982, Ap. J., 254, 349.

Orrall, F. Q. 1981, Solar Active Regions (Boulder: Colo. Assoc. Univ. Press).

Peres, G., Rosner, R., Serio, S., and Vaiana, G. S. 1982, Ap. J., 252, 791.

Raymond, J. C., Cox, D. P., and Smith, B. W. 1976, Ap. J., 204, 290.

Richtmyer, R. D., and Morton, K. W. 1967, Difference Methods for Initial-Value Problems (2nd ed., New York: Interscience Publishers).

Rosner, R., Tucker, W. H., and Vaiana, G. S. 1978, Ap. J., 220, 643.

Shoub, E. C. 1983, Ap. J., 266, 339.

Spitzer, L. 1962, Physics of Fully Ionized Gases (New York: Wiley Interscience).

Vernazza, J. E., Avrett, E. H., and Loesser, R. 1981, Ap. J. Suppl., 45, 635.

Vesecky, J. F., Antiochos, S. K., and Underwood, J. H. 1979, Ap. J., 233, 987.

Wragg, M. A., and Priest, E. R. 1982, Astron. Ap., 113, 269.

Figure Captions

Figure 1 Plots of free-surface and rigid-wall pressure perturbation (Figure 1a) and mass flux perturbation (Figure 1b) for the highly simplified model described in the text. The free-surface results are indicated by solid curves and the rigid-wall one by broken curves; the two types of modes are distinguishable only near the base, s = L.

Figure 2 The radiative loss coefficient of Raymond, Cox and Smith (1976) (broken line) and our analytic fit to it (solid line). The units in the figure are arbitrary.

Figure 3 The free-surface (solid curve) and rigid-wall (broken curve) growth rates for a series of static models with varying base temperatures and/or varying base depths.

Figure 4a Plot of lowest free-surface temperature perturbation (T_1/T_0) and rigid-wall perturbation (T_1P_0/T_0P_1) for the equilibrium model with $\delta = 5 \times 10^{-6}$ and a length $L = 14.2\ L_c$. The free-surface mode is indicated by a solid curve, and the rigid-wall one by a broken curve; they are indistinguishable in the corona and transition region. The scale of the abscissa is log (T_0) for $0 \leq s \leq 2L_c$, and s/L for $2L_c < s \leq L$.

Figure 4b Same as in Figure 4a but for the equlibrium model with $\delta = 10^{-3}$, and with an abscissa of log (T_0) for $0 \leq s/L \leq .94$ and log (s/L) for $.94 \leq s/L < 1$. Note that the rigid-wall amplitude is <u>negative</u> in the region $s/L > .94$.

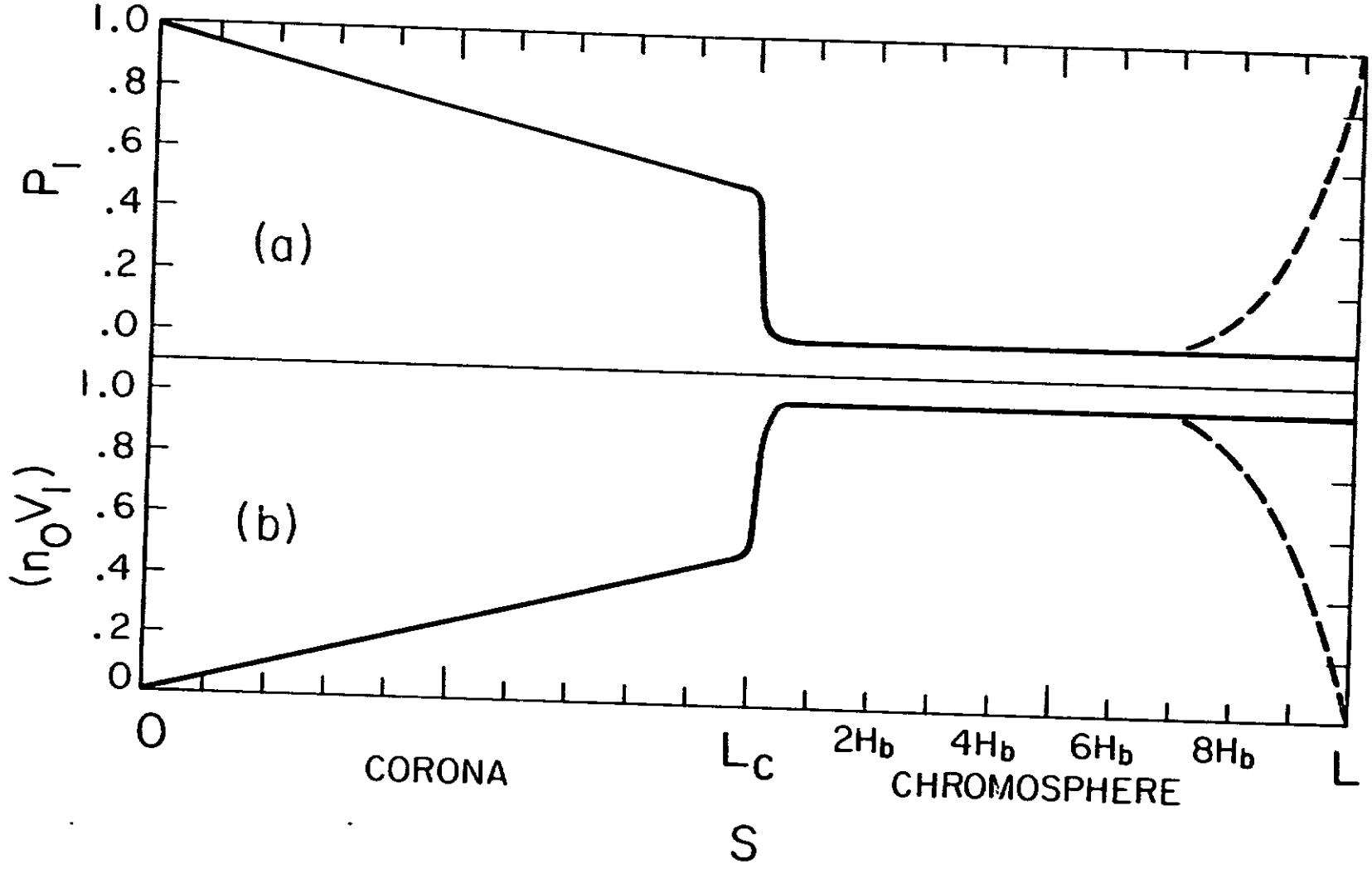
1.0
.8
.6
.4
.2
.0
P_-
(a)
1.0
.8
.6
.4
.2
0
$(n_o V_i)$
(b)
0
CORONA
L_c
$2H_b$
$4H_b$
$6H_b$
$8H_b$
CHROMOSPHERE
L
S

Figure 1

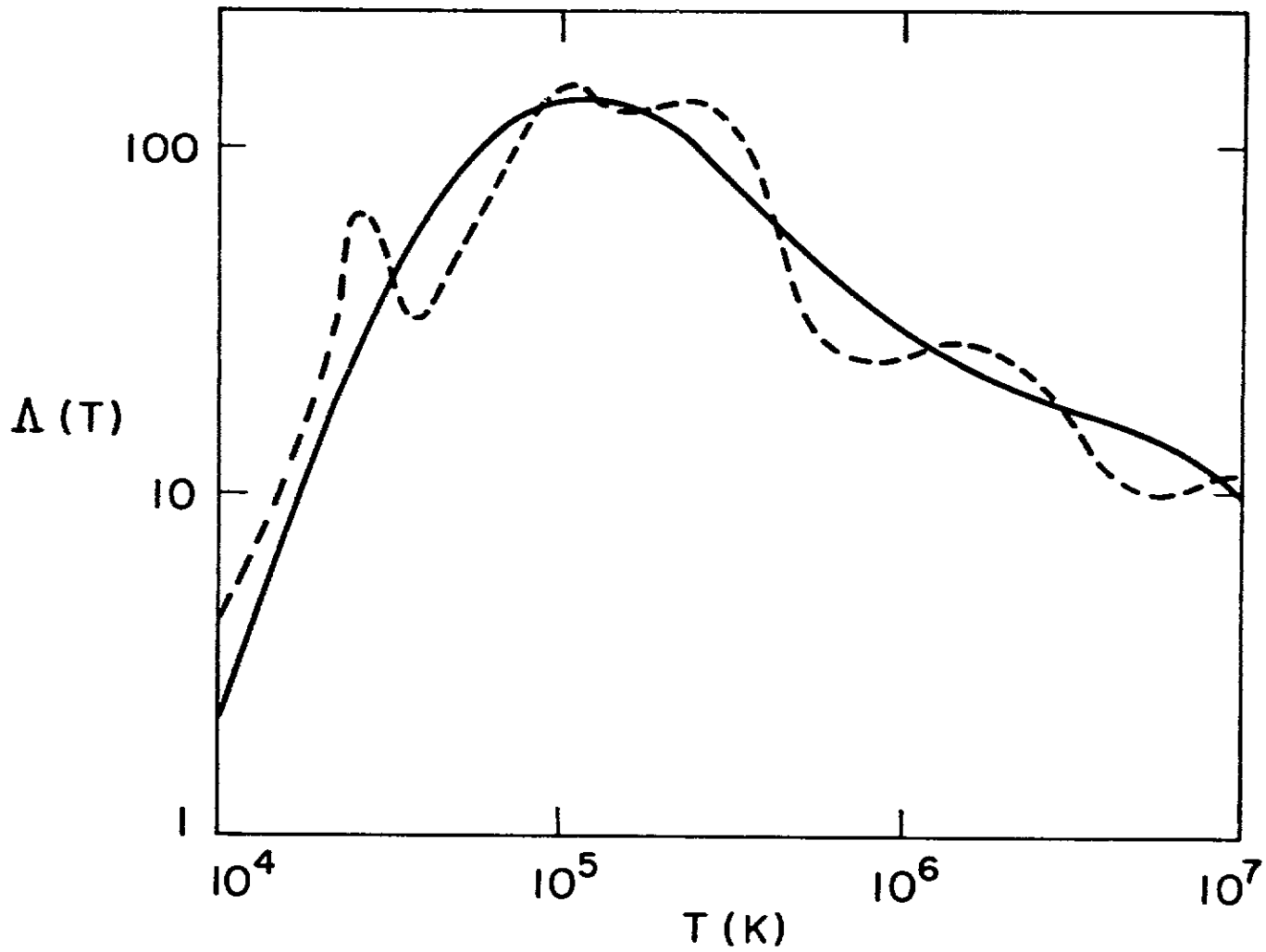

Figure 2

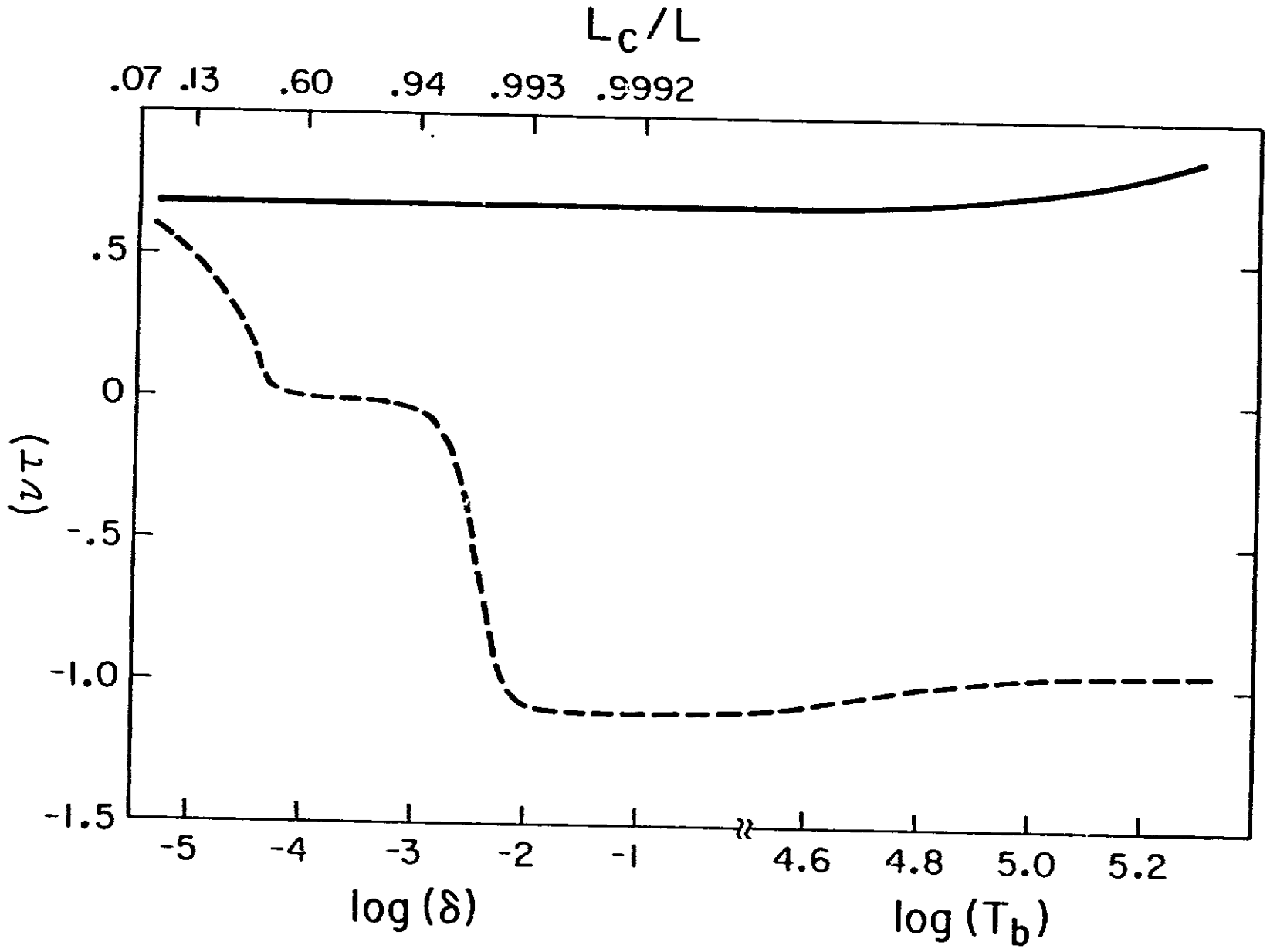
L_c/L
.07 .13 .60 .94 .993 .9992
.5
0
-.5
-1.0
-1.5
$(\tau\nu)$
-5 -4 -3 -2 -1
4.6 4.8 5.0 5.2
log (δ)
log (T_b)

Figure 3

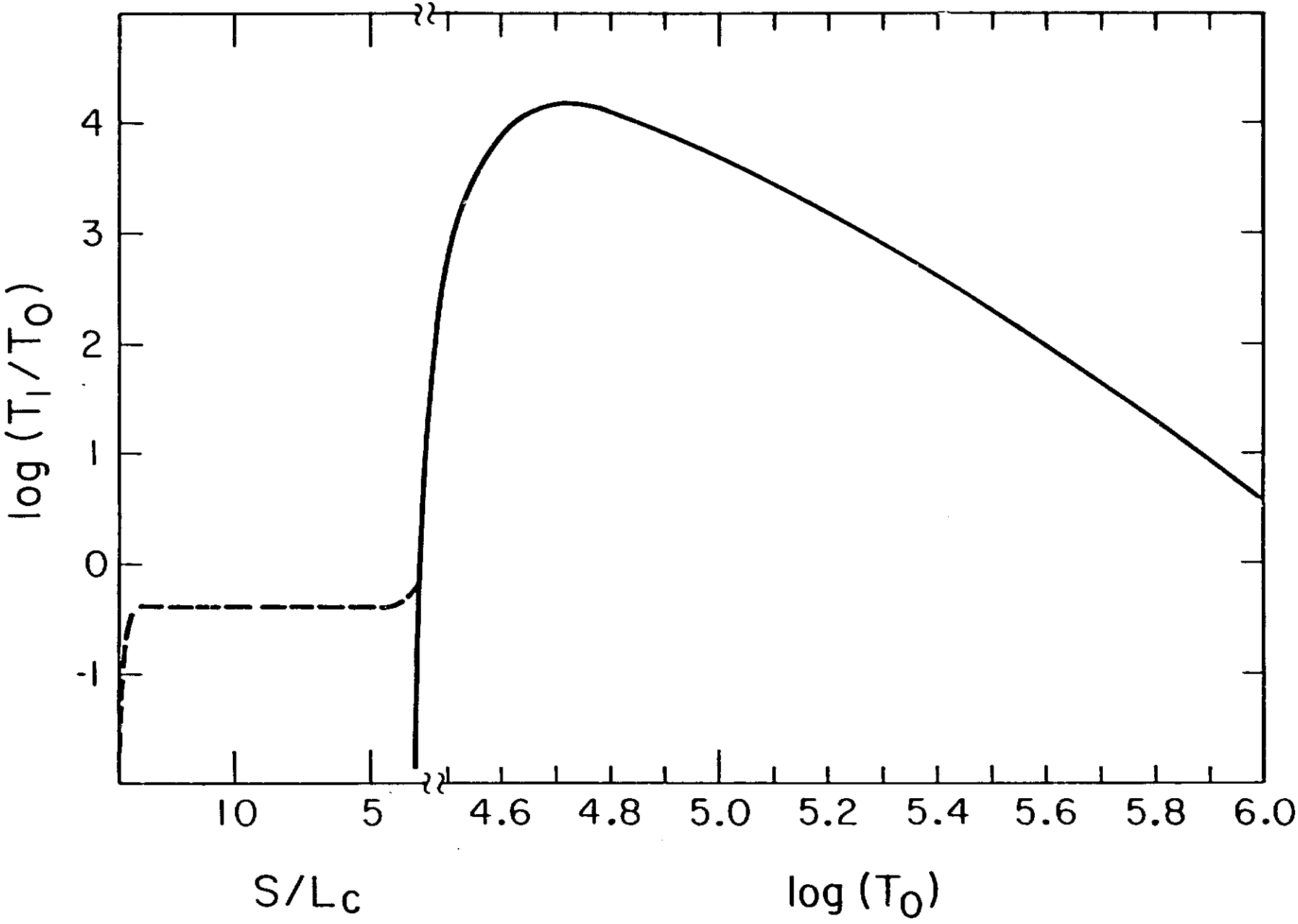

Figure 4a

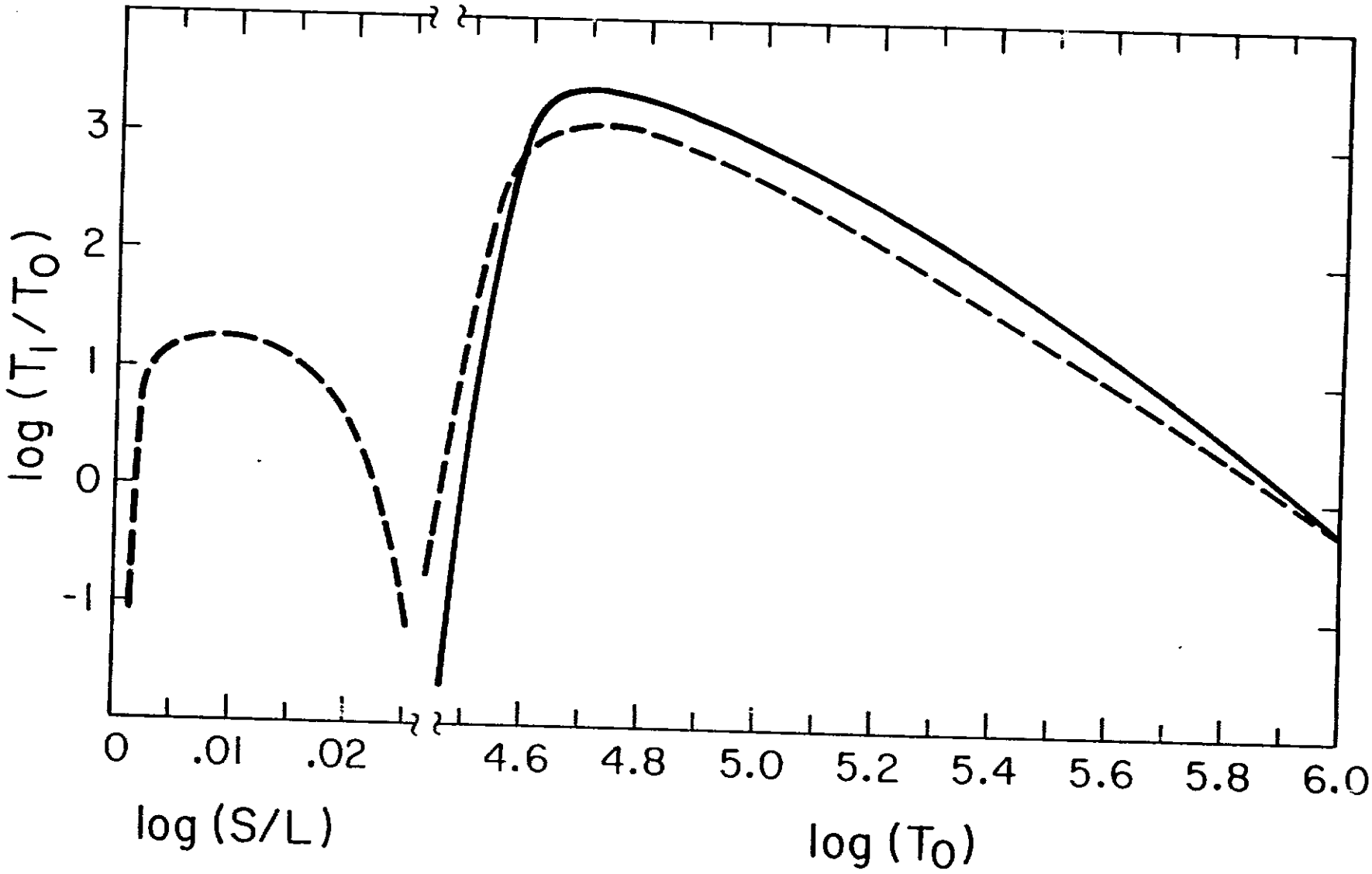

Figure 4b